THEME SPA.2013.1.1-05

EUCLEIA

(Grant Agreement 607085)

Eucleia

EUropean CLimate and weather Events: Interpretation and Attribution

Deliverable D7.*3*

Attribution of test drought

Deliverable Title	*attribution of test drought*	
Brief Description	*from DoW*	
WP number		
Lead Beneficiary	*Sonia Seneviratne & Mathias Hauser, ETHZ*	
Contributors	*Lukas Gudmundsson, ETHZ* *René Orth, ETHZ* *Karsten Haustein, University of Oxford*	
Creation Date Version Number Version Date		
Deliverable Due Date Actual Delivery Date	31. December 2016	
Nature of the Deliverable	x	*R - Report*
		P - Prototype
		D - Demonstrator
		O - Other
Dissemination Level/ Audience		*PU - Public*
	x	*PP - Restricted to other programme participants, including the Commission services*
		RE - Restricted to a group specified by the consortium, including the Commission services
		CO - Confidential, only for members of the consortium, including the Commission services

Version	**Date**	**Modified by**	**Comments**
1.0	22.12.2016	Mathias Hauser	
2.0	06.01.2017	Mathias Hauser	

Table of Contents

LIST OF TABLES

LIST OF FIGURES

1. Executive Summary

We provide hereafter an overview of the main results of this case study. This text is based on an article to be submitted soon (Hauser et al., in preparation).

Science on the role of anthropogenic influence on extreme weather events such as heat waves or droughts has evolved rapidly over the past years (Herring et al., 2015; Stott et al., 2016). This so called event attribution (Allen, 2003) compares the occurrence probability of an event in the present, factual world with the probability of the same event in a hypothetical, counterfactual world without human-induced climate change. Any such analysis necessarily faces multiple methodological choices including, but not limited to, the event definition, climate model configuration, and the design of the counterfactual world. Here, we explore the role of such choices for an attribution analysis of the European summer drought in 2015. We highlight that contrasting conclusions on the relevance of human influence are drawn depending on the chosen Global Circulation Model (GCM) and event attribution methodology. Assessments with observations indicate no human influence, whereas GCMs yield contrasting results spanning negative, no, and positive contribution of human-induced climate change. Our results highlight the need for a multi-model and multi- approach framework in event attribution research, especially for events with weak or no human influence such as regional droughts.

2. Project Objectives

With this deliverable, the project has contributed to the achievement of the following objectives (DOW, Section B1.1):

No.	Objective	Yes	No
1	Derive the requirements that targeted user groups (including regional stakeholders, re-insurance Companies, general public/media) have from attribution products and demonstrate the value to these users of the attribution products developed under EUCLEIA.		x
2	Develop experimental designs and clear ways of framing attribution studies in such a way that attribution products provide a fair reflection of current evidence on attributable risk.	x	
3	Develop the methodology for representing the level of confidence in attribution results so that attribution products can be trusted to inform decision making.	x	
4	Demonstrate the utility of the attribution system on a set of test cases of European weather extremes.	x	
5	Produce traceable and consistent attribution assessments on European climate and weather extremes on a range of timescales; on a fast-track basis in the immediate aftermath of extreme events, on a seasonal basis to our stakeholder groups, and annually to the BAMS attribution supplement.	x	

3. Detailed Report

It is expected that climate change will alter the occurrence of some meteorological extreme events. Yet, it is not possible to say that a specific, observed extreme event was caused by climate change (Allen, 2003; Stott et al., 2004). Due to the large internal variability of the climate system the investigated event could also have occurred in the absence of anthropogenic influence. The question that can be asked, however, is if the probability of the event has changed due to human influence. Event attribution quantifies this change with the Probability Ratio (Fischer and Knutti, 2015), PR = p_f / p_c, where p_f is the probability of the event in question in the factual world under climate change conditions and p_c the probability of the same event in the absence of climate change (see Figure 1).

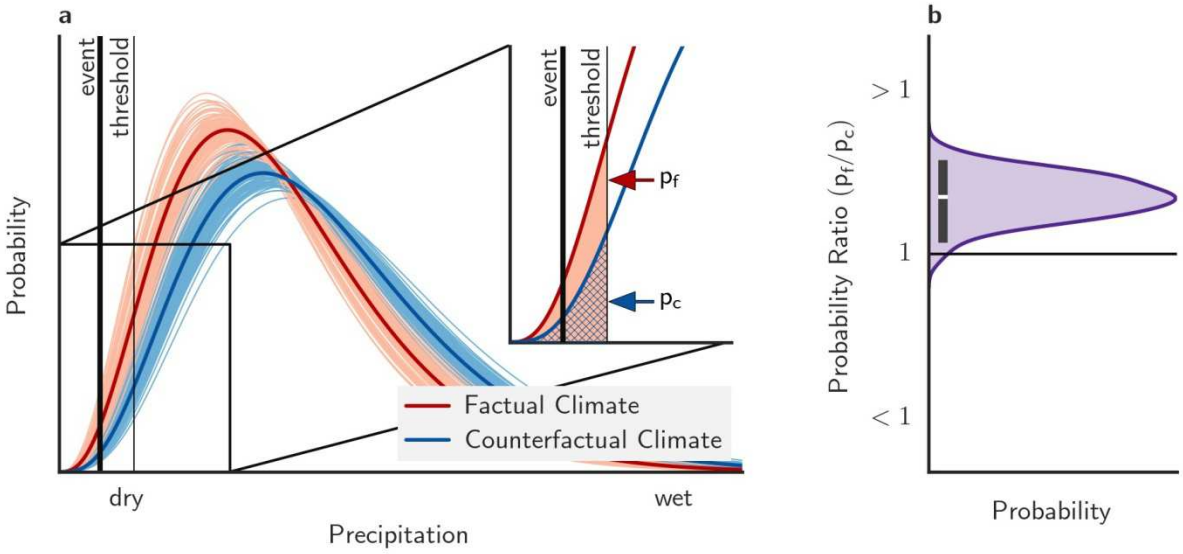

Figure 1: *Illustration of probabilistic event attribution and the Probability Ratio (PR). (a) Hypothetical Probability Density Functions (PDFs) of precipitation in the factual (red) and counterfactual (blue) climate. The thin, light lines indicate parameter uncertainty of the two PDFs. The magnitude of the investigated extreme event is indicated with the thick black line. To avoid a selection bias, we use the second largest event on the observational record as threshold (thin black line) for the calculation of p_f and p_C (inset). (b) PDF of the PR, taking the parameter uncertainty into account (magenta), 95 % credibility interval (black), and best estimate (median, white line).*

However, every event attribution study is based on a considerable number of methodological and technical choices, each potentially influencing the resulting attribution statement. We analyze the role of such choices for the European drought in 2015. The drought was characterized by very low precipitation during the summer months (June, July and August, JJA) in central Europe (Figure 2a). The cumulative JJA precipitation over a Central European region (defined in Seneviratne et al., 2012) did hit a new record low in 2015 and it was the driest summer in this region for at least 115

years (Figure 2b, Orth and Seneviratne, 2016), which resulted in significantly reduced surface water availability (Van Lanen et al., 2016; Laaha et al., 2016). While the extreme temperatures that went along with this event were successfully attributed to climate change (Dong et al., 2016; Sippel et al., 2016), an investigation of human influence on the drought is still lacking.

To obtain PR for this event, we need to estimate pf and pc, and their uncertainty (Figure 1). Therefore, we require the distribution of precipitation in a factual and a counterfactual world, respectively. From this distribution, we can then calculate pf and pc as the probability to stay below a precipitation threshold. As threshold we choose the second largest event on the observational record (Figure 2b) to avoid a selection bias (Stott et al., 2004). Thus, we do not estimate PR for the exact event, but for a class of events more severe than the driest observed year before 2015.

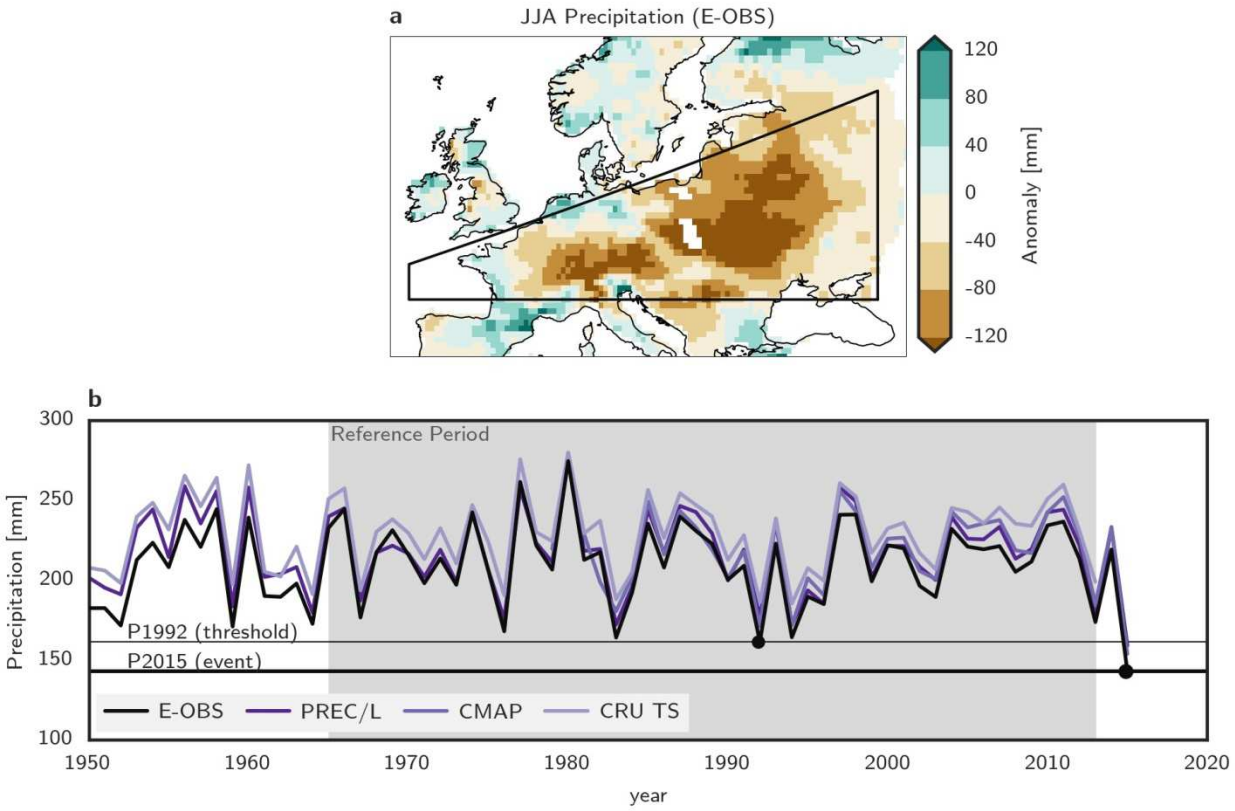

Figure 2: *(a) Map of precipitation anomaly over Europe for the summer (JJA) of 2015 (relative to 1965 to 2013). The black outline shows the study region (Seneviratne et al., 2012). (b) Absolute precipitation over the study region for four observational datasets. The horizontal lines denote the lowest (P2015, thick line) and second lowest (P1992, thin line) observed precipitation in the E-OBS dataset. We use P1992 as threshold to compute p_f and p_c (c.p. Figure 1). The gray shading indicates the reference period (1965 to 2013).*

For observation-based event attribution, no counterfactual world exists and the solution is to contrast a time period at the beginning of the observations, when human influence was still smaller, to a time period at its end, i.e. the current climate. This is often done in a regression framework to enhance the signal to noise ratio (see below, van Oldenborgh, 2007; Otto et al., 2012). However, observations constitute only a single realization of the climate system. This limitation can be approached through the use of GCMs that allow computing large ensembles. However, GCMs allow a large flexibility in their set up, which potentially influences the answers obtained from them. First, GCMs differ in the way they treat Sea Surface Temperatures (SSTs), which can either be interactively computed by the model or prescribed from observations. Second, GCMs can be forced with different boundary conditions, e.g. Carbon Dioxide (CO2). Given this flexibility, different ways to design the counterfactual world have been introduced (Table 1), which differ with respect to the greenhouse gas forcing, and the simulated time period. Third, the choice of the employed GCM may also influence the outcome of an attribution study.

***Table 1**: Overview of observation- and model-based event attribution methods. ΔSST indicate the changed SSTs due to climate change and is derived from CMIP5 models as ΔSSTs = $SST_{natural}$ - $SST_{historical}$, where $SST_{natural}$ and $SST_{historical}$ are the SSTs from natural and historical simulations, respectively.*

Data Basis	Name	Factual Climate (p_f) (with climate change)	Counterfactual Climate (p_c) (without climate change)
Models	PRES. vs. PAST	Anthropogenic forcing simulation of present-day period with: (1) Interactive SSTs (2) Observed SSTs	Anthropogenic forcing simulation of past time period ('1960s') with: (1) Interactive SSTs (2) Observed SSTs
	PRES. vs. NAT	Anthropogenic forcing simulation of present-day period with: (1) Interactive SSTs (2) Observed SSTs	Natural forcing simulations of present-day period with: (1) Interactive SSTs (2) Observed SSTs + ΔSST
	PRES. vs. piC	Anthropogenic forcing simulation of present-day period with: (1) Interactive SSTs	Natural forcing simulation of pre-industrial time period with: (1) Interactive SSTs
Observations	Trend-based	Present	Past (e.g. 1960s)

We start our assessment with GCM simulations with interactive SSTs, obtained from the Coupled Model Intercomparison Project Phase 5 (CMIP5, Taylor et al., 2012) archive. The factual climate (PRES) is estimated by simulations with greenhouse gas concentrations close to current-day levels, so called representative concentration pathway (RCP) 8.5 simulations. We use RCP 8.5 because the historical simulations only extend to 2005 and RCP 8.5 most closely matches the carbon dioxide observations (Peters et al., 2013). We choose a 20-year window (2006 to 2025) around the event. We contrast PRES with three counterfactual worlds. For the first we use historical simulations from the middle of the 20th Century (PAST), when the human imprint on the climate was smaller.

Thus, it is not a 'counterfactual' climate in the strict sense. For the second, we use historical natural simulations (NAT) that only include solar and volcanic forcings but no anthropogenic greenhouse gas emissions (1986 to 2005). The third counterfactual climate are freely evolving simulations with carbon dioxide concentrations appropriate for 1850, so called pre industrial Control (piC) simulations and we use 200 years of these simulations even if they are longer.

The spread between individual models is assessed by calculating a PR for each of these five GCMs that have at least five ensemble members. To get a 'global' attribution statement over several GCMs, it is common to combine CMIP5 members (Lewis and Karoly, 2013). PR is then calculated from the pooled data. Therefore, we select models by availability and use all CMIP5 members that submitted the necessary simulations. We present a total of three model pools: (i) every ensemble member of all available models (19 models, see Table S1), (ii) one ensemble member of all available models (to assign each model equal weight), and (iii) the five aforementioned individual models with five ensemble members. In total this yields 24 attribution statements, i.e. three counterfactual climates times eight model selections (five models plus three model pools).

Comparing the factual world to preindustrial control simulations (PRES vs. piC) almost unanimously indicates a strong human contribution to the drought of 2015 (Figure 3a). The pooled models have a PR of at least 1.5 (lower uncertainty bound), and three out of the five individual models show a significant probability increase. Thus, considering only PRES vs. piC one concludes that climate change has made the drought more likely. However, the result becomes less clear when we use historical natural simulations for the counterfactual climate (PRES vs. NAT). Only one of the individual models (CSIRO-Mk3-6-0) indicates a risk increase. Consequently, the PR for the pool of the five individual models is not significant. Combining all CMIP5 models, again yields PRs that suggest an anthropogenic influence on European drought risk. Finally, using a historical period (here: 1951 to 1970; PRES vs. PAST) only considers recent climate change, and we expect the smallest signal. Indeed, most of the models and all of the model pools indicate no human influence on precipitation. However, one of the models (CSIRO-Mk3-6-0) indicates a doubling of the drought risk (lower uncertainty bound) while another (GISS-E2-H) suggests half the drought risk (upper uncertainty bound). In essence, different subsets of CMIP5 models and counterfactual worlds produce different attribution statements with no consistency among them.

Next we assess GCM simulations with prescribed SSTs. We use two ensembles, the first from the

HadGEM3-A (Hadley Centre Global Environmental Model version 3-Atmosphere, Christidis et al., 2013; Ciavarella et al., in preparation) model, and the second from the weather at home (w@h Massey et al., 2015) project. The w@h employs the regional climate model HadRM3P over Europe, embedded in the global GCM HadAM3P. Observed SSTs are used to force simulations of the factual world. For the counterfactual world, an estimate of 'natural' SSTs with removed human signal is required. These are estimated by subtracting a modeled SST warming pattern (ΔSST) from the observations. ΔSST is the difference of historical natural to historical simulations for models from CMIP5. HadGEM3-A is forced with the Hadley Centre Sea Ice and Sea Surface Temperature (HadISST, Rayner et al., 2003) SST data set and the ΔSST pattern is a CMIP5 multi model mean from Christidis et al. (2013). w@h uses the Operational Sea Surface Temperature and Sea Ice Analysis (OSTIA, Donlon et al., 2012) dataset and ΔSST patterns are estimated from eleven individual CMIP5 models (Schaller et al., 2014, Table S3).

Comparing PRES vs. NAT on the basis of HadGEM3-A and the pooled w@h simulations yields a PR that is not distinguishable from one, and thus no attribution is possible (Figure 3b). The w@h simulations highlight the important role of different ΔSST patterns. Eight of the ΔSST patterns show no significant change in drought risk, but the other three indicate a reduced drought probability in the factual climate. The w@h simulations only start in 1985, therefore we cannot compare PRES vs. PAST in this model. In HadGEM3-A, PRES vs. PAST points to an increased drought risk due to climate change and is highly significant.

Finally, we perform an observation-based event attribution analysis for four different observational data sets (Figure 3c). We adjust all of them to E-OBS for consistency. Precipitation is regressed against global mean temperature, which is considered a proxy of climate change (van Oldenborgh, 2007; Gudmundsson and Seneviratne, 2016). Then we insert global mean temperature of 2015 and the mean of 1960 to 1969 into the regression to obtain p_f and p_c, respectively (see Methods). Due to the large internal variability, the short record length, and the absence of a clear precipitation trend, none of the datasets indicates a change in Central European drought risk, which is consistent with a previous assessment (Gudmundsson and Seneviratne, 2016).

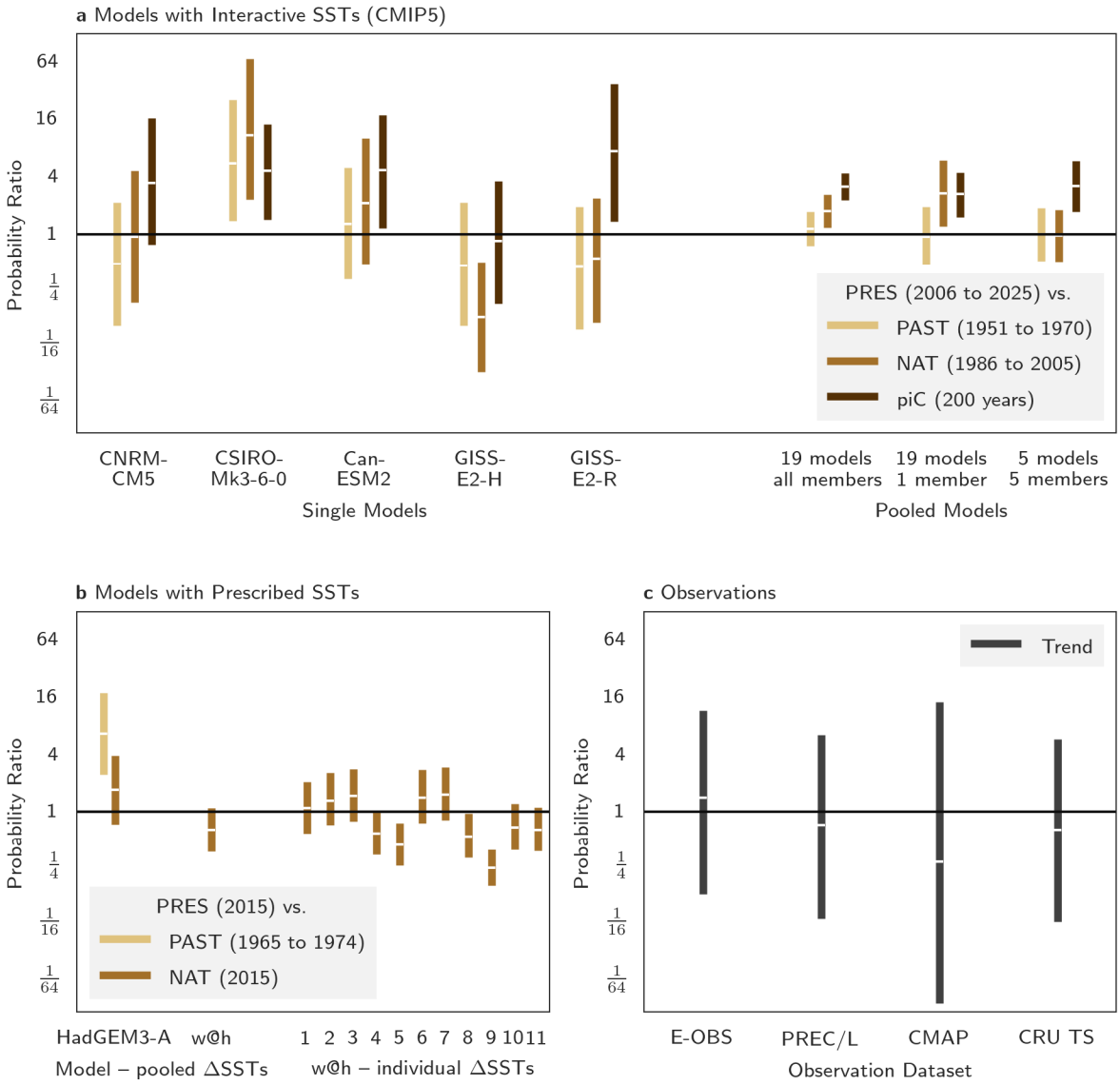

Figure 3: *Best estimate (median) and 95 % credibility interval of PR on a logarithmic axis. Dates in the legends indicate years used to estimate p_f and p_c. (a) Models with interactive SSTs from CMIP5 for three counterfactual climates (see Table 1). On the left are individual models with five ensemble members each. On the right three different sets of pooled models (Table S2). (b) Model simulations with prescribed SSTs. On the left HadGEM3-A and the pooled w@h simulations. On the right all eleven w@h simulations forced with individual ΔSST patterns, derived from CMIP5 models (Table S3). (c) PRs for four observational data sets.*

In this study we investigate if the 2015 meteorological drought in Central Europe was made more likely due to anthropogenic climate change. Our focus thereby was to include as many GCMs and counterfactual climates as possible, resulting in a wealth of different attribution statements. We find that the investigated drought could be more likely, less likely or unaffected by anthropogenic forcing. This ambiguity is also in line with other studies assessing droughts (King et al., 2014; Kelley et al., 2015; Rupp et al., 2015; Otto et al., 2015) and reiterates that the event attribution of droughts is inherently difficult. Any event attribution statement can – and will – critically depend on the researcher's decision and it is important to consolidate the methods and the terminology to better characterize and communicate uncertainties.

Methods

Data

We use four precipitation data sets: (i) the European Climate Assessment and Dataset (ECAD) E-OBS dataset (Haylock et al., 2008), (ii) the National Oceanic and Atmospheric Administration's (NOAA) PREcipitation REConstruction over Land (PREC/L, Chen et al., 2002), (iii) the Climate Prediction Center (CPC) Merged Analysis of Precipitation (CMAP, Xie and Arkin, 1997), and (iv) the Climatic Research Unit (CRU) Time Series datasets (CRU TS, Harris et al., 2014). As global mean temperature data set we employ the Goddard Institute for Space Studies (GISS) analysis of global surface temperature (GISTEMP, Hansen et al., 2010). We use simulations from 21 GCMs. Two GCMs, namely HadGEM3-A and the weather@home system (see main text), prescribe sea surface temperatures (SSTs). The others feature interactive SSTs and stem from the CMIP5 archive (Taylor et al., 2012).

We calculate cumulative precipitation on land for June, July and August (JJA), area-averaged over the Central European Special Report on Managing the Risks of Extreme Events and Disasters to Advance Climate Change Adaptation (SREX) region (Seneviratne et al., 2012) on the original model grid. All area-averaged data (models and observations) are bias corrected using a power transformation (e.g. Gudmundsson et al., 2012) to best match the cumulative density function of the E-OBS dataset for the period 1965 to 2013 (1985 to 2013 for the w@h simulations). This is done for every model individually, pooling all available ensemble members. The bias correction successfully adjusts the model simulations to the observations (see Supplementary Figure S1). The same bias correction is then applied to the counterfactual simulations.

Probability Ratio

For the GCM-based PR, we assume the precipitation data to follow a gamma distribution. We fit one gamma distribution to the simulated factual precipitation, and one to the counterfactual precipitation. These two gamma distributions are used to compute the probability to to fall below the chosen threshold (P1992, Figure 2), i.e. p_f and p_c, respectively. The assumption of gamma distributed data is visually assessed with quantile-quantile (QQ) plots of the historical simulations (see Supplementary Figure S2). The QQ plots give high confidence that the gamma distribution is appropriate to describe the used rainfall data. Only the w@h model data is stronger left skewed than a gamma distribution. We

calculate uncertainties in a Bayesian setting and use a Markov Chain Monte Carlo sampler that is affine-transformation invariant (Goodman and Weare, 2010; Foreman-Mackey et al., 2013) to estimate the parameters of the gamma distributions. Starting from noninformative priors, the converged posterior distributions of the parameters (50000 non-independent samples) give an estimate of the parameter uncertainty.

For the observation-based event attribution we follow a recent study (Gudmundsson and Seneviratne, 2016) and fit the precipitation data to a Generalized Linear Model (GLM) with global mean temperature as covariate, assuming a logarithmic link function and gamma distributed residuals. Global mean temperature (GISTEMP) is smoothed with a LOWESS filter (Cleveland, 1979) to minimize the influence of ENSO (van Oldenborgh, 2007). We use the global mean temperature of 2015 (for p_f) and the average temperature between 1960 and 1969 (for p0) as covariates to the GLM. The same MCMC algorithm as for the GCM-based PR is used to calculate the posterior distribution.

Acknowledgments We acknowledge the E-OBS dataset from the EU-FP6 project ENSEMBLES (http://ensembles-eu.metoffice.com) and the data providers in the ECA&D project (http://www.ecad.eu)

Supplementary Material

Table S1: *CMIP5 models and ensemble members used for the pooled estimate of PR (in Figure 3a)*

Models	Factual	Counterfactual		
	PRE	PAST	NAT	piC
BNU-ESM	1	1	1	1
CCSM4	6	6	4	1
CESM1-CAM5	3	3	3	1
CNRM-CM5	5	5	6	1
CSIRO-Mk3-6-0	10	10	5	1
CanESM2	5	5	5	1
FGOALS-g2	1	1	3	1
GFDL-CM3	1	1	3	1
GFDL-ESM2M	1	1	1	1
GISS-E2-H	5	5	10	1
GISS-E2-R	5	5	10	1
HadGEM2-ES	4	4	4	1
IPSL-CM5A-LR	4	4	3	1
IPSL-CM5A-MR	1	1	3	1
MIROC-ESM	1	1	3	1
MIROC-ESM-CHEM	1	1	1	1
MRI-CGCM3	1	1	1	1
NorESM1-M	1	1	1	1
bcc-csm1-1	1	1	1	1

Table S2: *Best estimate and uncertainty of the PR for simulations with interactive SSTs (Figure 3a). # ens. is the number of ensemble members. The 2.5th, 50th, and 97.5th percentile is indicated by p2.5, p50, and p97.5, respectively. Bold numbers indicate a significant PR at the 5 % level.*

Models	# ens	HIST vs. PAST			HIST vs. NAT			HIST vs. piC		
		$p_{2.5}$	p_{50}	$p_{97.5}$	$p_{2.5}$	p_{50}	$p_{97.5}$	$p_{2.5}$	p_{50}	$p_{97.5}$
CNRM-CM5	5	0.19	0.9	4.4	0.10	0.5	2.4	0.68	3.5	15.1
CSIRO-Mk3-6-0	5	**2.14**	**10.7**	**60.**	**1.30**	**5.5**	**25.**	**1.37**	**4.4**	**15.6**
CanESM2	5	0.51	2.1	9.2	0.31	1.3	5.3	**1.34**	**4.9**	**17.8**
GISS-E2-H	5	**0.03**	**0.1**	**0.5**	0.09	0.5	2.2	0.18	0.8	3.5
GISS-E2-R	5	0.13	0.6	2.7	0.10	0.5	1.8	**1.57**	**7.6**	**39.9**
all (19)	all	0.76	1.1	1.7	**1.16**	**1.7**	**2.6**	**2.24**	**3.1**	**4.4**
all (19)	1	0.45	0.9	1.9	**1.22**	**2.7**	**6.0**	**1.51**	**2.6**	**4.5**
pooled (5)	5	0.52	1.0	1.8	0.51	1.0	1.8	**1.71**	**3.1**	**5.6**

Table S3: *Best estimate and uncertainty of the PR for simulations with prescribed SSTs (Figure 3b). ΔSST pattern indicates the model used to calculate the natural SSTs and # ens. is the number of ensemble members. The 2.5th, 50th, and 97.5th percentile is indicated by $p_{2.5}$, p_{50}, and $p_{97.5}$, respectively. Bold numbers indicate a significant PR at the 5 % level. w@h has 3777 ensemble members in the historical simulation and HadGEM3-A has 105.*

Models	ΔSST pattern	# ens.	HIST vs. PAST			HIST vs. NAT		
			$p_{2.5}$	p_{50}	$p_{97.5}$	$p_{2.5}$	p_{50}	$p_{97.5}$
HadGEM3-A	Multi Model Mean	105	**2.49**	**6.7**	**17.**	0.7	1.7	4.2
w@h	Pooled	5181	—	—	—	0.4	0.6	1.1
w@h	CNRM_CM5	468	—	—	—	0.6	1.1	2.1
w@h	IPSL_CM5A_MR	464	—	—	—	0.7	1.3	2.4
w@h	CanESM2	470	—	—	—	0.8	1.5	3.0
w@h	CSIRO_Mk3	477	—	—	—	0.3	0.6	1.0
w@h	MIROC_ESM	442	—	—	—	**0.3**	**0.4**	**0.8**
w@h	OSTIA	480	—	—	—	0.8	1.4	2.7
w@h	CCSM4	481	—	—	—	0.8	1.6	3.1
w@h	IPSL_CM5A_LR	472	—	—	—	**0.3**	**0.6**	**1.0**
w@h	GISS_E2_R	478	—	—	—	**0.2**	**0.3**	**0.4**
w@h	GISS_E2_H	469	—	—	—	0.4	0.7	1.2
w@h	GFDL_CM3	480	—	—	—	0.4	0.6	1.2

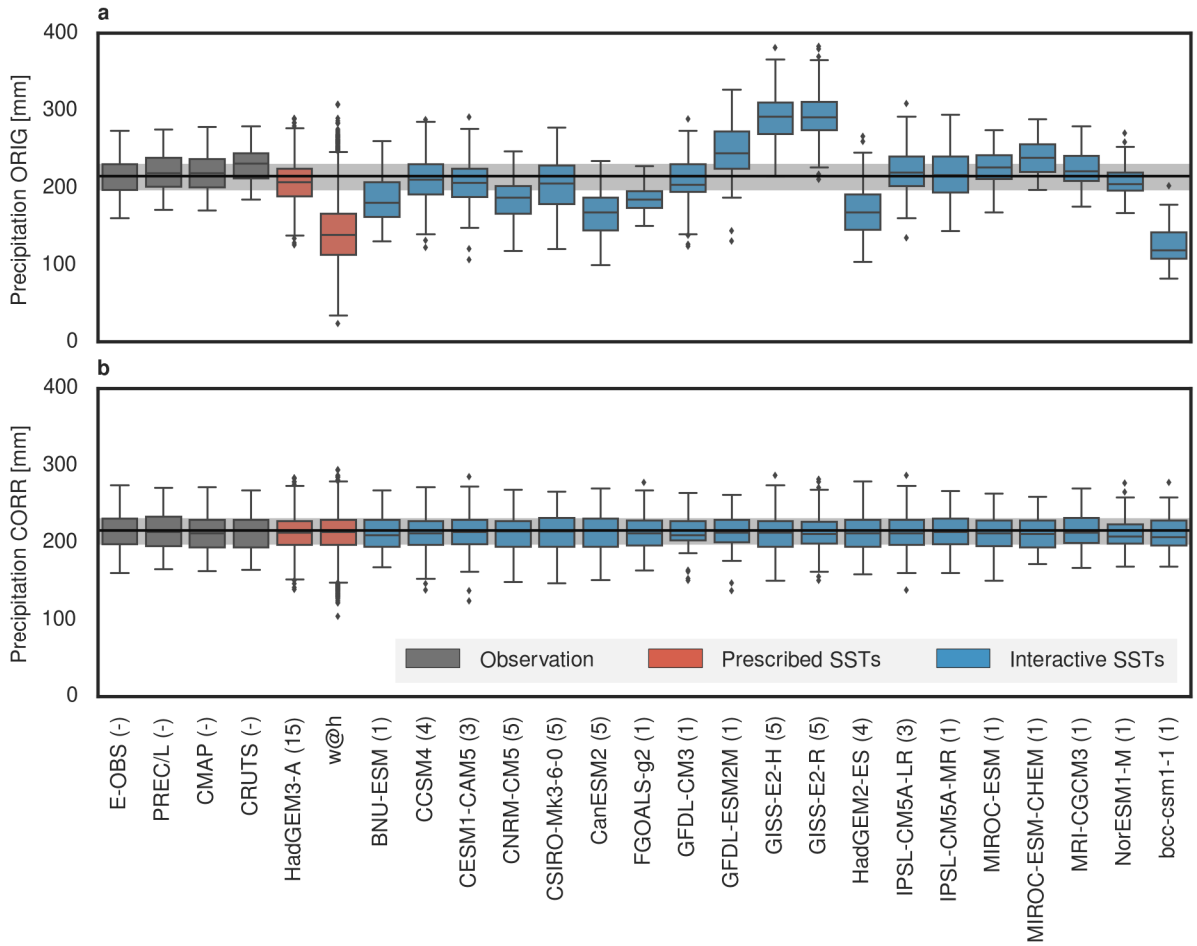

Figure S1: *Boxplot of observations and historical GCM simulations from 1965 to 2013 (1985 to 2013 for w@h). (a) Raw data before bias correction. (b) Bias corrected data. All observations and GCM simulations are adjusted to E-OBS using a power transformation. The black line shows the median and the light gray shading the interquartile range of E-OBS. Digit in the labels indicate the number of historical ensemble members.*

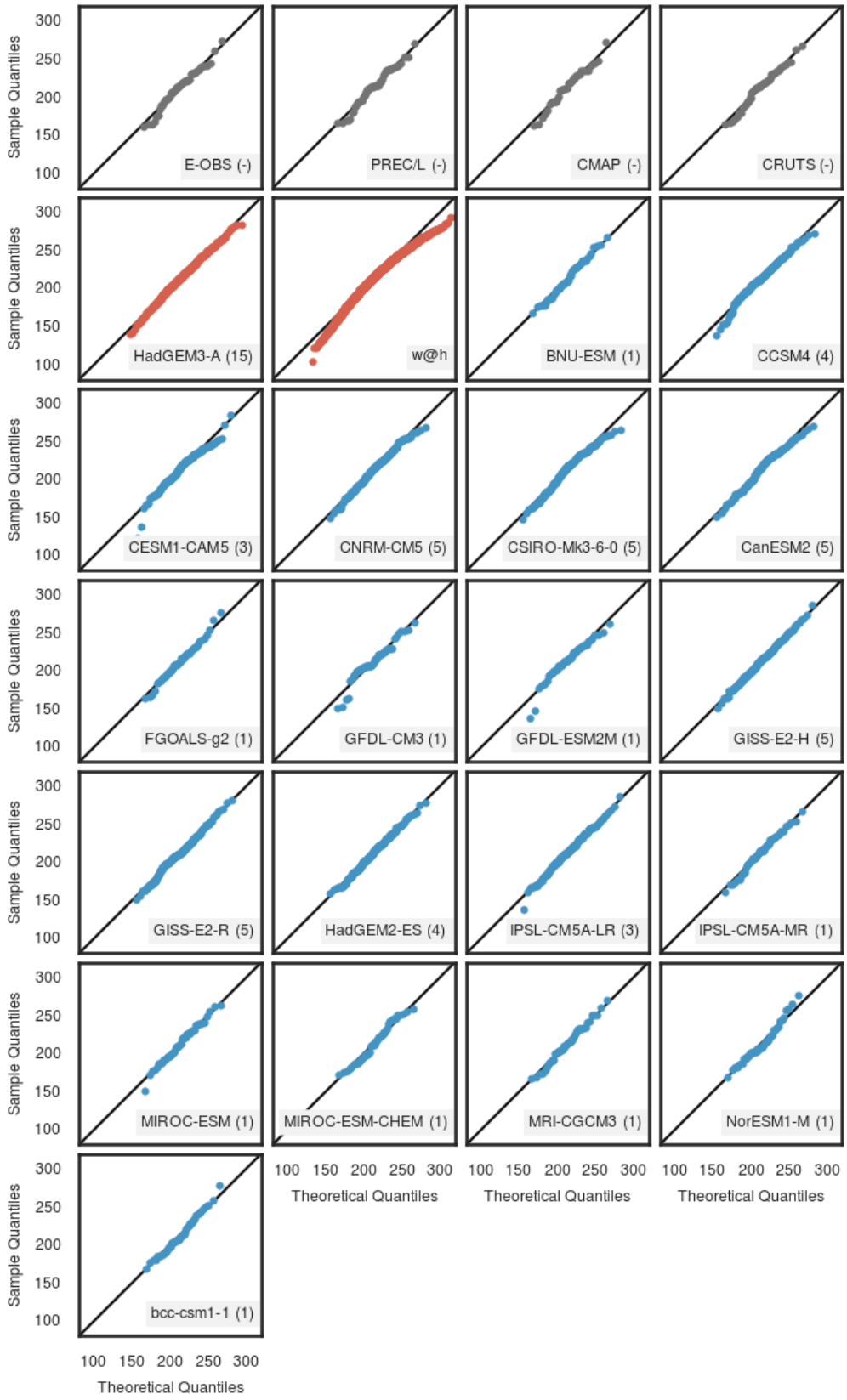

Figure S2: *Quantile-quantile (QQ) plot of observations and historical GCM simulations. Assesses if the gamma distribution provides an appropriate description of the data.*

References

Allen, M. 2003. Liability for climate change. Nature 421, 891–892.

Chen, M., P. Xie, J. Janowiak, and P. Arkin. 2002. Global land precipitation: A 50-yr monthly analysis based on gauge observations. Journal of Hydrometeorology 3, 249–266.

Christidis, N., P. A. Stott, A. A. Scaife, A. Arribas, G. S. Jones, D. Copsey, J. R. Knight, and W. J. Tennant. 2013. A New HadGEM3-A-Based System for Attribution of Weather- and Climate-Related Extreme Events. Journal of Climate 26, 2756–2783.

Ciavarella et al. in preparation. The HadGEM3-A N216 system for probabilistic attribution of extreme weather and climate events. Cleveland, W. 1979. Robust Locally Weighted Regression And Smoothing Scatterplots. Journal Of The American Statistical Association 74, 829–836.

Dong, B., R. Sutton, L. Shaffrey, and L. Wilcox. 2016. The 2015 European Heat Waves. Bulletin of the American Meteorological Society 97, S57–S62.

Donlon, C. J., M. Martin, J. Stark, J. Roberts-Jones, E. Fiedler, and W. Wimmer. 2012. The Operational Sea Surface Temperature and Sea Ice Analysis (OSTIA) system. Remote Sensing of Environment 116, 140–158.

Fischer, E. M., and R. Knutti. 2015. Anthropogenic contribution to global occurrence of heavy-precipitation and high-temperature extremes. Nature Climate Change 5, 560+.

Foreman-Mackey, D., D. W. Hogg, D. Lang, and J. Goodman. 2013. emcee: The MCMC Hammer. Publications of the Astronomical Society of the Pacific 125, 306–312.

Goodman, J., and J. Weare. 2010. Ensemble samplers with affine invariance. Communications in Applied Mathematics and Computational Science 5, 65–80.

Gudmundsson, L., and S. I. Seneviratne. 2016. Anthropogenic climate change affects meteorological drought risk in Europe. Environmental Research Letters.

Gudmundsson, L., J. B. Bremnes, J. E. Haugen, and T. Engen-Skaugen. 2012. Technical Note: Downscaling RCM precipitation to the station scale using statistical transformations - a comparison of methods. Hydrology and Earth System Sciences 16, 3383–3390.

Hansen, J., R. Ruedy, M. Sato, and K. Lo. 2010. Global Surface Temperature Change. Reviews of Geophysics.

Harris, I., P. D. Jones, T. J. Osborn, and D. H. Lister. 2014. Updated high-resolution grids of monthly climatic observations - the CRU TS3.10 Dataset. International Journal of Climatology 34, 623–642.

Hauser et al. in preparation. Methodological and model uncertainty in event attribution: the European drought of 2015.

Haylock, M. R., N. Hofstra, A. M. G. K. Tank, E. J. Klok, P. D. Jones, and M. New. 2008. A European daily high-resolution gridded data set of surface temperature and precipitation for 1950-2006. Journal of Geopyhsical Research-Atmospheres.

Herring, S. C., M. P. Hoerling, J. P. Kossin, T. C. Peterson, and P. A. Stott. 2015. Explaining Extreme Events Of 2014 From A Climate Perspective. Bulletin of the American Meteorological Society.

Kelley, C. P., S. Mohtadi, M. A. Cane, R. Seager, and Y. Kushnir. 2015. Climate change in the Fertile Crescent and implications of the recent Syrian drought. Proceedings of the National Academy of Sciences of the United States of America 112, 3241–3246.

King, A. D., D. J. Karoly, M. G. Donat, and L. V. Alexander. 2014. Climate Change Turns Australia's 2013 Big Dry into a Year Of Record- breaking Heat. Bulletin of the American Meteorological Society 95, S41–S45.

Laaha, G., T. Gauster, L. M. Tallaksen, J.-P. Vidal, K. Stahl, C. Prudhomme, B. Heudorfer, R. Vlnas, M. Ionita, H. A. J. Van Lanen, M.-J. Adler, L. Caillouet, C. Delus, M. Fendekova, S. Gailliez, J. Hannaford, D. Kingston, A. F. Van Loon, L. Mediero, M. Osuch, R. Romanowicz, E. Sauquet, J. H. Stagge, and W. K. Wong. 2016. The european 2015 drought from a hydrological perspective. Hydrology and Earth System Sciences Discussions 2016, 1–30.

Lewis, S. C., and D. J. Karoly. 2013. Anthropogenic contributions to Australia's record summer temperatures of 2013. Geophysical Research Letters 40, 3705–3709.

Massey, N., R. Jones, F. E. L. Otto, T. Aina, S. Wilson, J. M. Murphy, D. Hassell, Y. H. Yamazaki, and M. R. Allen. 2015. weather@home—development and validation of a very large ensemble modelling system for probabilistic event attribution. Quarterly Journal of the Royal Meteorological Society 141, 1528–1545.

Orth, R., and S. Seneviratne. 2016. Soil moisture and sea surface temperatures similarly important for climate in the warm season.. Journal of Climate. in review.

Otto, F. E. L., C. A. S. Coelho, A. King, E. C. De Perez, Y. Wada, G. J. van Oldenborgh, R. Haarsma, K. Haustein, P. Uhe, M. van Aalst, J. A. Aravequia, W. Almeida, and H. Cullen. 2015. Factors Other than Climate Change, Main Drivers of 2014/15 Water Shortage in Southeast Brazil. Bulletin of the American Meteorological Society 96, S35–S40.

Otto, F. E. L., N. Massey, G. J. van Oldenborgh, R. G. Jones, and M. R. Allen. 2012. Reconciling two approaches to attribution of the 2010 Russian heat wave. Geophysical Research Letters 39, L04702.

Peters, G. P., R. M. Andrew, T. Boden, J. G. Canadell, P. Ciais, C. Le Quere, G. Marland, M. R. Raupach, and C. Wilson. 2013. Commentary: The challenge to keep global warming below 2 degrees C. Nature Climate Change 3, 4–6.

Rayner, N., D. Parker, E. Horton, C. Folland, L. Alexander, D. Rowell, E. Kent, and A. Kaplan. 2003. Global analyses of sea surface temperature, sea ice, and night marine air temperature since the late nineteenth century. Journal of Geopyhsical Research-Atmospheres.

Rupp, D. E., S. Li, N. Massey, S. N. Sparrow, P. W. Mote, and M. Allen. 2015. Anthropogenic influence on the changing likelihood of an exceptionally warm summer in Texas, 2011. Geophysical Research Letters 42, 2392–2400.

Schaller, N., F. E. L. Otto, G. J. van Oldenborgh, N. R. Massey, S. Sparrow, and M. R. Allen. 2014. The Heavy Precipitation Event Of May-june 2013 In The Upper Danube And Elbe Basins. Bulletin of the American Meteorological Society 95, S69–S72.

Seneviratne, S., N. Nicholls, D. Easterling, C. Goodess, S. Kanae, J. Kossin, Y. Luo, J. Marengo, K. McInnes, M. Rahimi, M. Reichstein, A. Sorteberg, C. Vera, and X. Zhang. 2012. Managing the Risks of Extreme Events and Disasters to Advance Climate Change Adaptation. In: Changes in climate extremes and their impacts on the natural physical environment.. Pp. 109–230. A Special Report of Working Groups I and II of the Intergovernmental Panel on Climate Change.

Sippel, S., F. E. L. Otto, M. Flach, and G. J. van Oldenborgh. 2016. The Role of Anthropogenic Warming in 2015 Central European Heat Waves. Bulletin of the American Meteorological Society 97, S51–S56.Stott, P. A., N. Christidis, F. E. L. Otto, Y. Sun, J.-P. Vanderlinden, G. J. van Oldenborgh, R. Vautard, H. von Storch, P. Walton, P. Yiou, and F. W. Zwiers. 2016. Attribution of extreme weather and climate-related events. Wiley Interdisciplinary Reviews-climate Change 7, 23–41. Stott, P., D. Stone, and M. Allen. 2004. Human contribution to the European heatwave of 2003. Nature 432, 610–614.

Taylor, K. E., R. J. Stouffer, and G. A. Meehl. 2012. An overview of CMIP5 and the experiment design. Bulletin of the American Meteorological Society 93, 485–498.

Van Lanen, H. A. J., G. Laaha, D. G. Kingston, T. Gauster, M. Ionita, J.-P. Vidal, R. Vlnas, L. M. Tallaksen, K. Stahl, J. Hannaford, C. Delus, M. Fendekova, L. Mediero, C. Prudhomme, E. Rets, R. J. Romanowicz, S. Gailliez, W. K. Wong, M.-J. Adler, V. Blauhut, L. Caillouet, S. Chelcea, N. Frolova, L. Gudmundsson, M. Hanel, K. Haslinger, M. Kireeva, M. Osuch, E. Sauquet, J. H. Stagge, and A. F. Van Loon. 2016. Hydrology needed to manage droughts: the 2015 European case. Hydrological Processes 30, 3097–3104.

van Oldenborgh, G. J. 2007. How unusual was autumn 2006 in Europe?. Climate of the Past 3, 659–668.

Xie, P., and P. Arkin. 1997. Global precipitation: A 17-year monthly analysis based on gauge observations, satellite estimates, and numerical model outputs. Bulletin of the American Meteorological Society 78, 2539–2558.

4. Lessons Learnt

Positive

We were able to bring together a wide range of climate models to obtain a thorough uncertainty quantification of the probability ratio for the European drought of 2015.

Negative

Every simulation has its own setup and it is difficult to bring all of them to a common framework.

5. Links Built

In this case study we were able to build links to many other deliverables (D) and work packages (WP) within EUCLEIA. We employed observational datasets from D6.1 (E-OBS and GISTEMP). By assessing the probability ratio for different counterfactual worlds and analogues we investigated the question of framing for the drought (D5.3). More specifically, we used the following methods described in D5.3 (see there for details): (i) the CMIP5 method, (ii) very large ensembles of regional climate models with observed SSTs and SST response patterns from CMIP5 (i.e. the weather at home approach), and (iii) the empirical method. We also analyzed model output from HadGEM3-A and therefore greatly profited from WP8 and D6.3.